Catal Lett (2008) 120:65–70
DOI 10.1007/s10562-007-9250-2

The Effect of Different Active Sites on the Catalytic Activity of Fe-ZSM-5 Zeolite for N_2O Direct Decomposition

Quanhui Guo · Biaohua Chen · Yingxia Li · Jianwei Li

Received: 8 July 2007 / Accepted: 21 August 2007 / Published online: 11 September 2007

Abstract Fe-modified ZSM-5 zeolites (Si/Al = 25) were prepared by adopting the liquid ion-exchange method with nitrate and oxalate of iron as Fe precursors and their catalytic performance was studied in the N_2O decomposition reaction. The results of FT-IR and H_2-TPR investigations indicated that (i) part of the iron ions could replace Brönsted acid protons at the straight channel wall (α sites), intersection of straight and sinusoidal channels (β sites), and sinusoidal channel wall (γ sites) within the ZSM-5 zeolite; and (ii) different Fe precursors gave rise to various distributions of α, β, and γ sites. We observed that the Fe-ZSM-5 catalyst prepared with iron oxalate as Fe precursor outperformed the ones prepared with iron nitrate as Fe precursor in the direct decomposition of N_2O. Furthermore, the catalytic activity of iron ions located at the α sites was higher than those of iron ions located at the β and γ sites.

Keywords Fe-ZSM-5 · Zeolite · N_2O decomposition · Brönsted acid · Ion exchange

1 Introduction

N_2O has been considered as an environmental pollutant due to its destroying the ozone layer and inducing the greenhouse effect. At present, the atmospheric N_2O mainly comes from agriculture, transportation, and industrial manufacture. The removal of the N_2O from industrial waste gases has received much attention. The direct decomposition of N_2O over metal-modified zeolites represents the simplest and most attractive pathway for the abatement of N_2O, since it require no addition of any reducing agent and the only products are environment-friendly N_2 and O_2 [1–4].

Liquid ion-exchange is the most commonly used method to prepare metal-exchanged zeolites. In recent years, the studies have shown that iron ions at the Brönsted acid sites exhibited good catalytic activity in N_2O direct decomposition though the amount of iron ions introduced to the ZSM-5 zeolite via the liquid ion-exchange method was lower (Fe/Al $< 50\%$) [5–7]. Pieterse and van den Brink [8] investigated the preparation methods of Fe-modified ZSM-5 and beta zeolites systematically and proposed that the pH value of the suspension of the iron precursor and the zeolite during liquid ion-exchange is a key factor in generating a high-performance catalyst for N_2O decomposition. They found that the Fe-ZSM-5 zeolites prepared with different iron precursors showed different catalytic activity, such a phenomenon was attributed to the difference in pH value during ion-exchange. In addition, the pore structure of the zeolite also influences the metal ion loading. It is well known that ZSM-5 zeolite with MFI topology possesses two intersection pore systems. There are three types of Brönsted acid sites in ZSM-5 zeolite: (i) straight channel wall, (ii) intersection of straight and sinusoidal channels, and (iii) sinusoidal channel wall, designated as the α, β, and γ sites, respectively. By means of diffuse reflectance UV–vis and near-IR spectroscopic techniques, Wichterlová and his co-workers [9, 10] disclosed that metal ions could locate at the different Brönsted acid sites in ZSM-5 zeolite with a rise in metal ion loading. However, the effect of iron

Q. Guo · B. Chen · Y. Li · J. Li
State Key Laboratory of Chemical Resource Engineering, Beijing University of Chemical Technology, Beijing 100029, China

Q. Guo (✉)
College of Chemistry and Chemical Engineering, Henan University, Kaifeng 475001, China
e-mail: 2004080033@grad.buct.edu.cn

ions at different Brönsted acid sites in ZSM-5 zeolite on the catalytic activity is still not clear for the direct decomposition of N_2O.

In this paper, Fe-modified ZSM-5 catalysts with different iron ion loadings were prepared by the ion-exchange strategy with $Fe(NO_3)_3 \cdot 9H_2O$ and $Fe_2(C_2O_4)_3 \cdot 5H_2O$ as the Fe precursors. The aim is to investigate the effect of iron ions loaded at different Brönsted acid sites on the catalytic performance for N_2O direct decomposition.

2 Experimental

2.1 Catalyst Preparation

Commercial zeolite H-ZSM-5 (Si/Al = 25) was used as the starting material. The Fe-modified ZSM-5 zeolites were prepared by mixing appropriate amounts of commercial H-ZSM-5 zeolite, $Fe(NO_3)_3 \cdot 9H_2O$ or $Fe_2(C_2O_4)_3 \cdot 5H_2O$, and deionized water in a three-necked bottle under the conditions of stirring and refluxing at 100 °C for 3 h. The resulting mixture were filtered and recovered with deionized water. This washing procedure was repeated three times and then the wet products were dried in an oven at 110 °C for 12 h. Finally, the obtained Fe-ZSM-5 zeolites were calcined at 540 °C for 4 h. The catalysts prepared through the liquid ion-exchange method with different iron ion loadings are listed in Table 1. The samples are denoted as FX-Y_{-Z}, where the X stands for different Fe precursors (N = $Fe(NO_3)_3 \cdot 9H_2O$, O = $Fe_2(C_2O_4)_3 \cdot 5H_2O$), the Y is the Si/Al ratio, and the Z is the theoretical loading of iron ions.

2.2 Catalyst Characterization

The iron ion contents of all the samples were determined by ICP elemental analysis (Spectroflame D). Temperature-programmed reduction in H_2 (H_2-TPR) was carried out using Thermo TPDRO 1100 Series. According to the method described in the literature [11], the samples were heated at 500 °C for 90 min in a mixture of 10% O_2–90% He (v/v) and then cooled to room temperature. Then, the 5% H_2–95% He (v/v) mixed gas was passed over the sample at 40 °C for 20 min prior to initiating a temperature ramp of 20 °C/min.

Pyridine sorption FT-IR was recorded on Nicolet NEXUS 470 FT-IR with DTGS detector at room temperature to characterize the acidity of the samples. IR spectra were measured on zeolites in the form of self-supporting wafers ($\sim$10 mg/cm^2). Sample wafers pretreated in vacuum at 400 °C for 1 h to remove adsorbed H_2O and then cooled to room temperature for pyridine adsorption. Afterwards, the wafers were heated to 200 °C to remove the physically adsorbed pyridine molecules. The spectra were recorded with a spectral resolution of 4 cm^{-1} and 64 scans. The value of the integrated molar absorption coefficients ε_B for pyridine bound to Brönsted acid sites is equal to 1.13 cm/μmol [12].

Infrared spectra were recorded on a Bruker TENSOR 27 FTIR spectrometer using a MCT liquid nitrogen cooled detector and with a heatable cell with CaF_2 windows to characterize the bands assigned to the hydroxyl stretching and the perturbed anti-symmetric T–O–T vibrations of iron-ions loaded in Fe-ZSM-5 zeolite channels [13]. IR spectra measurements after pretreatments were collected with a spectral resolution of 2 cm^{-1} and 128 scans at room temperature.

Table 1 Results of elemental analysis of the samples

Sample	Fe-ICP (wt. %)	Fe/Al	Brönsted acid amount (mmol/g)	Percentage of Brönsted acid protons displaced (%)
H-ZSM-5	0.067	0.016	0.503	
FN-$25_{-0.25}$	0.23	0.07	0.479	4.8
FN-$25_{-0.5}$	0.45	0.14	0.453	10
FN-$25_{-1.0}$	0.98	0.30	0.397	21
FO-$25_{-0.2}$	0.20	0.06	0.475	5.6
FO-$25_{-1.0}$	0.96	0.29	0.377	25

2.3 Catalytic Evaluation

The N_2O direct decomposition reaction was performed in a continuous fixed-bed micro-reactor (Φ 21 × 3 × L 450 mm) at atmospheric pressure. One gram of the catalyst was pressed into a wafer, and then crashed, ground, and sieved to 40–60 mesh particles. Prior to the catalytic measurement, the catalysts were activated in He at 500 °C for 5 h, followed by cooling to the reaction temperature in the same atmosphere. The reactants with N_2O/He molar ratio = 35/65 were continuously passed through the catalyst bed with GHSV = 4000 h^{-1} (gas hourly space velocity). N_2O, N_2 and O_2 were analyzed on-line with a gas chromatography equipped with a thermal conductivity detector (TCD).

3 Results

3.1 ICP Results and Acidity Characterization

As seen in Table 1, Brönsted acid amounts of the Fe-modified ZSM-5 prepared with different iron precursors decreased gradually with increasing the iron ion loading, a

result due to the replacement of a part of the Brönsted acid protons by iron ions during the liquid ion-exchange process.

3.2 Locations of Iron Ions

The infrared spectra in the hydroxyl stretching region of the samples are showed in Fig. 1. Bands were observed at 3740, 3670, and 3610 cm^{-1}. The band at 3740 cm^{-1} has been assigned to hydroxyl stretching at Si(OH) groups at crystal terminations [11, 14] while the band at 3670 cm^{-1} has been assigned to hydroxyl stretching on Fe^{3+} species (Fe–OH) [14]. The band at 3610 cm^{-1} was due to the hydroxyl stretching of Brönsted acid groups [11, 14]. The principal effect of increased Fe loading was a decrease in the intensity of the band at 3610 cm^{-1}, giving direct evidence for the displacement of Brönsted acid protons by iron ions.

FT-IR spectra were recorded to investigate the perturbed T–O–T anti-symmetric vibrations of the iron ions in the channel of Fe-ZSM-5 in the 980–910 cm^{-1} region and the results are shown in Figs. 2 and 3. As seen in Fig 2, at low iron loading (Fe/Al = 0.07), the bands were observed at 923 and 927 cm^{-1}. The intensities of these bands were strengthened and an additional strong band at 954 cm^{-1} appeared when the Fe/Al ratio was ≤0.14. At a Fe/Al ratio of 0.3, the intensities of the bands at 923, 927, and 954 cm^{-1} increased with the rise in iron loading. These results are in agreement with those reported in literature [9, 13]. The bands at 954, 927, and 923 cm^{-1} have been attributed to the perturbed T-O-T anti-symmetric vibrations of iron ions located at the wall of the straight channels (α sites), the intersection of straight and sinusoidal channels (β sites), and the wall of sinusoidal channels (γ sites) in the MFI-type ZSM–5 zeolite, respectively [9]. From the results of FT-IR studies, one can realize that iron ions could locate at the α, β, and γ sites of the ZSM-5 zeolite channels. In the case of the Fe-ZSM-5 zeolites prepared with $Fe(NO_3)_3 \cdot 9H_2O$ as Fe precursor, the iron ions could locate at the β and γ sites at a iron loading of 0.07, but they would locate at the α sites when the iron loading increased.

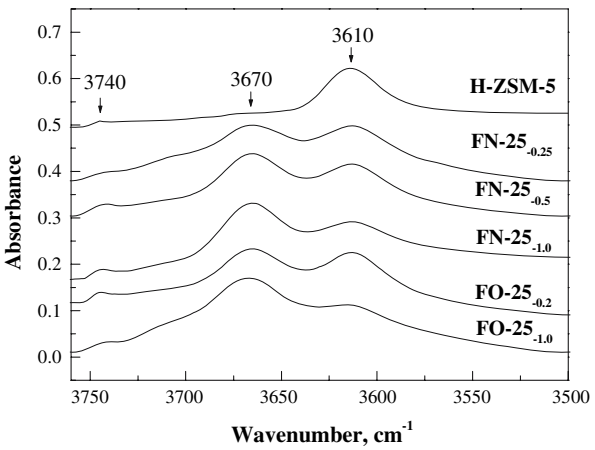

Fig. 1 FT-IR spectra of hydroxyl stretching over H-ZSM-5 and Fe-ZSM-5 zeolites. Pretreatment conditions: 400 °C, 1 h in vacuum

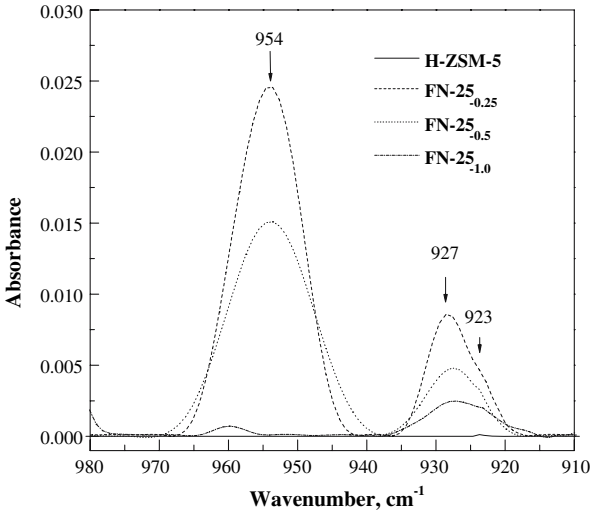

Fig. 2 FT-IR spectra of perturbed T–O–T anti-symmetric mode over FN zeolites prepared with $Fe(NO_3)_3 \cdot 9H_2O$ as Fe precursor. Pretreatment conditions: 400 °C, 1 h in vacuum

Figure 3 shows the FT-IR spectra of the Fe-modified ZSM-5 samples prepared with $Fe_2(C_2O_4)_3 \cdot 5H_2O$ as Fe precursor. For the FO-$25_{-0.2}$ sample, a strong band at 954 cm^{-1} was detected. With a rise in iron loading (i.e., the FO-$25_{-1.0}$ sample), the intensity of the band at 954 cm^{-1} increased. For the both samples, almost no changes in intensity of the 927 and 923 cm^{-1} bands were observed. These results indicated that for the Fe-ZSM-5 samples

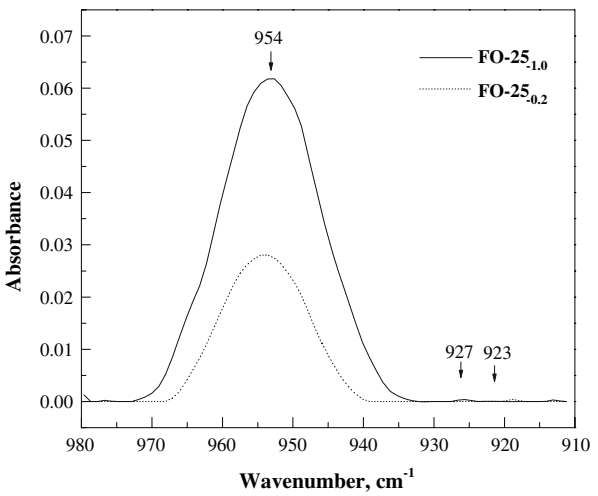

Fig. 3 FT-IR spectra of perturbed T–O–T anti-symmetric mode over FO zeolites prepared with $Fe_2(C_2O_4)_3 \cdot 5H_2O$ as Fe precursor. Pretreatment conditions: 400 °C, 1 h in vacuum

obtained with $Fe_2(C_2O_4)_3 \cdot 5H_2O$ as Fe precursor, iron ions mainly occupied the α sites of the zeolitic straight channels.

3.3 Reducibility

Shown in Figs. 4 and 5 are the H_2-TPR profiles of the Fe-ZSM-5 zeolites obtained with different iron precursors. It is observed that the FN-$25_{-0.25}$ sample exhibited one main H_2 reduction band at 464 °C, which was due to the reduction of Fe^{3+} ions located at the Brönsted acid sites of ZSM-5 zeolite [15]. A molar ratio of consumed H_2 to Fe on Fe-ZSM-5 could to be 0.5 on the basis of the equation $Fe^{3+} + ½H_2 \rightarrow Fe^{2+} + H^+$. These results indicated that iron species on Fe-ZSM-5 zeolites existed as Fe^{3+} ions after O_2 pretreatment. In addition, it should be noted that the position of this reduction band gradually shifted to a lower temperature with the rise in iron ion loading. Kunimori et al. [15] prepared Fe-ZSM-5 zeolite through liquid ion-exchange using $FeSO_4 \cdot 7H_2O$ as iron precursor. They also observed that more reducible Fe ions were formed over Fe-ZSM-5 with higher Fe loading. The reason could be explained as follows: the iron ions fills primarily β and γ sites for the sample with low Fe loading and then as the iron loading increases the fraction of Fe occupying α sites increases. According to the literature [11], the iron ions locating in the α sites is the most easily reduced in H_2 from Fe^{3+} to Fe^{2+}. For the samples prepared with $Fe_2(C_2O_4)_3 \cdot 5H_2O$ as iron precursor, there was only one reduction band at 415 °C (Fig. 5) although the two samples possessed different iron ion loadings, since iron ions mainly occupies the α sites of ZSM-5 zeolite.

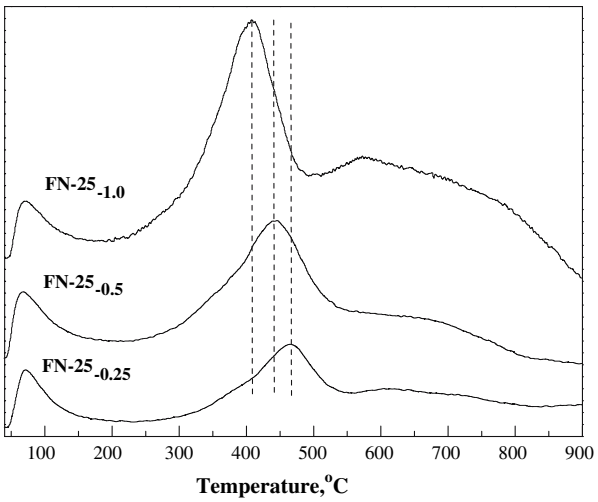

Fig. 4 H_2-TPR profiles of the Fe-ZSM-5 zeolites prepared with $Fe(NO_3)_3 \cdot 9H_2O$ as Fe precursor

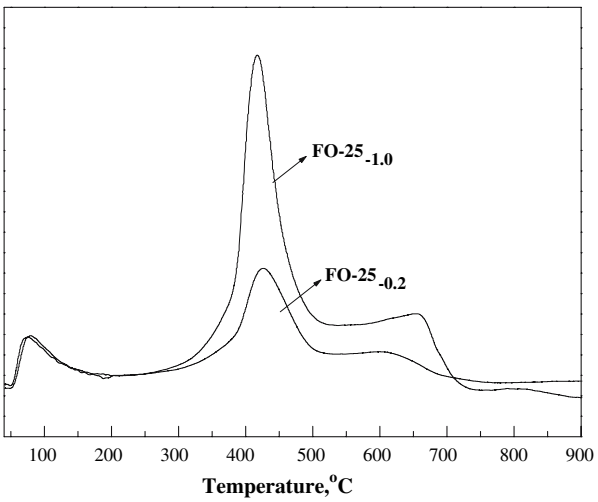

Fig. 5 H_2-TPR profiles of the Fe-ZSM-5 zeolites prepared with $Fe_2(C_2O_4)_3 \cdot 5H_2O$ as Fe precursor

3.4 Catalytic Activity

Figure 6 shows the N_2O conversion versus reaction temperature over the Fe-ZSM-5 (Si/Al = 25) zeolitic catalysts prepared with different iron precursors. As seen in Fig. 6, N_2O conversion increased with the rise in reaction temperature over all the catalysts; simultaneously, the catalytic activity enhanced with increasing the iron loading. By

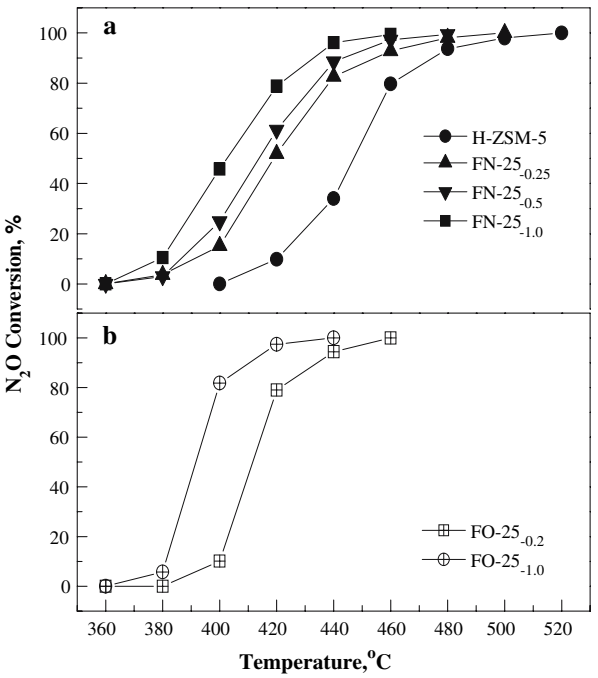

Fig. 6 Catalytic activities of the Fe-ZSM-5 zeolites prepared with $Fe(NO_3)_3 \cdot 9H_2O$ and $Fe_2(C_2O_4)_3 \cdot 5H_2O$ as Fe precursors for the decomposition of N_2O under the reaction condition of 1 atm and space velocity 4000 h^{-1}

comparing the catalytic performance of the samples prepared with different iron precursors, one can realize that the Fe-ZSM-5 catalyst prepared with $Fe_2(C_2O_4)_3 \cdot 5H_2O$ as Fe precursor outperformed its counterpart obtained with $Fe(NO_3)_3 \cdot 9H_2O$ as Fe precursor.

4 Discussion

4.1 Effect of Iron Ions on the N_2O Decomposition

Up to now, the nature of the active species of Fe-ZSM-5 zeolites has not been completely elucidated. After investigating the Fe-ZSM-5 zeolitic catalysts prepared via the liquid ion-exchange pathway by using different iron precursors, Melián-Cebrera et al. [7], Pirngurber et al. [16] and van den Brink et al. [17] pointed out that the charge-balancing iron cations loaded on the ZSM-5 zeolite were responsible for N_2O direct decomposition. In our experiments, the results of pyridine sorption (Table 1) and FT-IR spectra of hydroxyl stretching of the Brönsted acid sites (Fig. 1) indicated that a part of iron ions were loaded on the zeolite by replacing the Brönsted acid proton H. Taking into account the conversion of N_2O and the percentage of Brönsted acid protons displaced (Table 1), we concluded that the iron ions located at the Brönsted acid sites were the active component in the direct decomposition of N_2O.

4.2 Effect of Different Iron Precursors

Bell et al. [11] have studied the iron ions introduced to the α, β, and γ sites of ZSM-5 prepared through the ion-exchange method by means of H_2-TPR, and observed that these iron ion species possessed different oxidation–reduction abilities, in which the one located at the α sites was the most easily reduced. In the present work, the H_2-TPR results showed that the position of reduction peak shifted to the lower temperature with increasing the iron ion loading in Fe-ZSM-5 prepared with $Fe(NO_3)_3 \cdot 9H_2O$ as iron precursor, indicating that the iron ions preferentially located at the β and γ sites. In the case of the Fe-ZSM-5 zeolites prepared with $Fe_2(C_2O_4)_3 \cdot 5H_2O$ as iron precursor, there was no shift in reduction peak (at 415 °C) for the different Fe^{3+}-containing ZSM-5 samples. This result indicated that iron ions mainly located at the α sites of the ZSM-5 straight channels. In addition, the infrared spectra investigations also give the direct evidence for different Fe precursors lending to different distributions of α, β, and γ sites. At present, it is not well clear why different Fe precursors lead to various distributions of α, β, and γ sites. Recently, Nechita et al. [18] also prepared Fe-ZSM-5 zeolite with low iron loading through liquid ion-exchange by $Fe_2(C_2O_4)_3 \cdot 6H_2O$ as iron precursor. They found that the $[Fe(C_2O_4)]^+$ (oxalatoiron(III) ion) was involved in the exchange process. However, the hydroxorion (III) complexes as $(Fex(OH)y)^{3x-y}$ were in solution during the exchange process using $Fe(NO_3)_3 \cdot 9H_2O$ as precursor [8]. Thus, we speculate that such a phenomenon might be associated with the different hydrolysis products derived from $Fe(NO_3)_3 \cdot 9H_2O$ and $Fe_2(C_2O_4)_3 \cdot 5H_2O$ and the special pore structure of ZSM-5.

4.3 Effect of Iron Ions at Different Acid Sites on Catalytic Activity

The FT-IR results showed that iron ions could locate at the α, β, and γ sites of ZSM-5 channels, respectively. But in the case of Fe-ZSM-5 prepared with $Fe(NO_3)_3 \cdot 9H_2O$ as Fe precursor, iron ions mainly located at the β and γ sites when iron loading was lower (Fe/Al = 0.07). However, the catalytic activity of the FN-$25_{-0.25}$ sample was dramatically improved compared to that of the commercial H-ZSM-5 sample. And the ICP results (Table 1) showed that iron ion content in H-ZSM-5 was very low (0.067%). These results suggest that the iron ions located at the β and γ sites of the ZSM-5 channels have the ability to directly decompose N_2O molecules. In the case of the Fe-ZSM-5 zeolite prepared with $Fe_2(C_2O_4)_3 \cdot 5H_2O$ as Fe precursor, however, iron ions mainly located at the α sites, and the catalytic activity of the Fe-ZSM-5 sample enhanced with the rise in Fe^{3+} loading. It indicates that the iron ions located at the α sites also have the ability to decompose N_2O to N_2 and O_2.

In experiments, the results of catalytic evaluation showed that the catalytic activity enhanced with increasing the iron loading (Fig. 6). These suggested that the catalytic activity of Fe-modified zeolite was related to the iron loading in the N_2O decomposition reaction. In addition, the catalytic activities of Fe-modified zeolites prepared with different iron precursors were different. For example, although the FO-$25_{-0.2}$ and FN-$25_{-0.25}$ samples exhibited rather similar catalytic activities below 400 °C, the former catalyst performed obviously superior to the latter one above 400 °C. This indicated that the Fe-ZSM-5 catalyst prepared with $Fe_2(C_2O_4)_3 \cdot 5H_2O$ as Fe precursor outperformed its counterpart obtained with $Fe(NO_3)_3 \cdot 9H_2O$ as Fe precursor. Noticed that the values of percentage of Brönsted acid protons displaced for FO-$25_{-0.2}$ and FN-$25_{-0.25}$ were close (Table 1) and the iron ions located at the Brönsted acid sites were the active component in the direct decomposition of N_2O. These suggested that the amounts of the active component were close for the FO-$25_{-0.2}$ and FN-$25_{-0.25}$ samples. However, the results of FT-IR investigation showed that different Fe precursors lead to various distributions of α, β, and γ sites. For the Fe-ZSM-5 samples

obtained with $Fe_2(C_2O_4)_3 \cdot 5H_2O$, iron ions mainly occupied the α sites while in the case of the Fe-ZSM-5 zeolites prepared with $Fe(NO_3)_3 \cdot 9H_2O$, part of iron ions located at the β and γ sites. Thus, it can be stated that the catalytic activity mainly depends on the location of iron ions and the iron ions located at the α sites showed higher catalytic activity than their counterparts located at the β and γ sites.

As illustrated in the H_2-TPR study, the iron ions located at the α sites could be reduced at lower temperatures. It indicates that the charge-balancing iron ions in ZSM-5 could undergo the auto-reduction after pretreatment in He at 500 °C. Moreover, Pirngruber et al. [19] believed that the first step of N_2O decomposition is the interaction of Fe^{2+} with N_2O to give a Fe^{3+}–O^- species, which then transforms into the Fe^{2+}–peroxo complex; O_2 desorption occurs via the recombination of two peroxo species migrated through the iron ion sites. Since the rate-determining step in N_2O directs decomposition is the removal of the generated oxygen from the Fe ion sites [16, 20], the higher the reducibility of the Fe species the better the catalytic performance. In addition, iron ions located at the α sites of the ZSM-5 straight channels may be more accessible to N_2O molecules [21]. Therefore, the iron ions located at the α sites showed higher catalytic activity than those located at the β and γ sites.

5 Conclusions

The Fe-ZSM-5 zeolites with different Fe ion loadings were prepared by the liquid ion-exchange method using $Fe(NO_3)_3 \cdot 9H_2O$ and $Fe_2(C_2O_4)_3 \cdot 5H_2O$ as Fe precursors. For the direct decomposition of N_2O, the catalytic activities of the Fe-ZSM-5 samples prepared with $Fe_2(C_2O_4)_3 \cdot 5H_2O$ as Fe precursor were higher than those of the Fe-modified ZSM-5 samples obtained with $Fe(NO_3)_3 \cdot 9H_2O$ as Fe precursor. The iron ions located at the α sites were more active than the ones located at the β and γ sites for the addressed reaction.

Acknowledgement This work was supported by NSFC (No. 20625621).

References

1. Fanson PT, Stradt MW, Lauterbach J, Delgass WN (2002) Appl Catal B 38:331
2. Øygarden AH, Pérez-Ramírez J (2006) Appl Catal B 65:163
3. Kawi S, Liu SY, Shen S-C (2001) Catal Today 68:237
4. da Cruz RS, Mascarenhas AJS, Andrade HMC (1998) Appl Catal B 18:223
5. Pirngruber GD, Pieterse JAZ (2006) J Catal 237:237
6. Pirngurber GD, Luechinger M, Roy PK, Cecchetto A, Smirniotis P (2004) J Catal 224:429
7. Melián-Cebrera I, Espinosa S, Groen JC, v/d Linden B, Kapteijn F, Moulijn JA (2006) J Catal 238:250
8. Pieterse JAZ, Booneveld S, van den Brink RW (2004) Appl Catal B 51:215
9. Wichterlová B, Sobalík Z, Dědeček J (2003) Appl Catal B 41:97
10. Dědeček J, Wichterlová B (1999) J Phys Chem B 103:1462
11. Lobree LJ, Hwang I-C, Reimer JA, Bell AT (1999) J Catal 186:242
12. Selli E, Forni L (1999) Micropor Mesopor Mater 31:129
13. Sobalík Z, Tvarůžková Z, Wichterlová B (1998) J Phys Chem B 102:1077
14. Nobukawa T, Sugawara K, Okumura K, Tomishige K, Kunimori K (2007) Appl Catal B 70:342
15. Yoshida M, Nobukawa T, Ito S-I, Tomishige K, Kunimori K (2004) J Catal 223:454
16. Pirngruber GD, Roy PK, Prins R (2007) J Catal 246:147
17. van den Brink RW, Booneveld S, Pels JR, Bakker DF, Verhaak MJFM (2001) Appl Catal B 32:73
18. Nechita M-T, Berlier G, Ricchiardi G, Bordiga S, Zecchina A (2005) Catal Lett 103:33
19. Roy PK, Pirngruber GD (2004) J Catal 227:164
20. Smeets PJ, Groothaert MH, van Teeffelen RM, Leeman H, Hensen EJM, Schoonheydt RA (2007) J Catal 245:358
21. Yu M, Kustov KA, Christiansen SE, Leth KT, Rasmussen SB, Christensen CH (2006) Catal Commun 7:705